1   A meiotic drive element in the maize pathogen *Fusarium verticillioides* is located within a 102-

2   kb region of chromosome V.

3

4   Jay Pyle*, Tejas Patel*, Brianna Merrill*, Chabu Nsokoshi*, Morgan McCall*, Robert H.

5   Proctor[†], Daren W. Brown[†,2], and Thomas M. Hammond*[,2]

6

7   *School of Biological Sciences, Illinois State University, Normal, IL 61790, and [†]National

8   Center for Agricultural Utilization Research, USDA-ARS, Peoria, IL 61604

9

13

14   [2]Corresponding authors: National Center for Agricultural Utilization Research 1815 N

15   University St., Peoria, IL 61604. E-mail: daren.brown@ars.usda.gov; Illinois State University,

16   School of Biological Sciences, Julian Hall 210, Campus Box 4120, Normal, IL 61790. E-mail:

17   tmhammo@ilstu.edu.

18

1

19   Running title

20   A meiotic drive element in Fusarium

21

22   KEYWORDS

23   genomic conflict, mapping, meiotic drive, fungi, spore killing

24

25   [2]Corresponding authors: National Center for Agricultural Utilization Research 1815 N

26   University St., Peoria, IL 61604. E-mail: daren.brown@ars.usda.gov; Illinois State University,

27   School of Biological Sciences, Julian Hall 210, Campus Box 4120, Normal, IL 61790. E-mail:

28   tmhammo@ilstu.edu.

29

30

31 **ABSTRACT**

32 *Fusarium verticillioides* is an agriculturally important fungus because of its association with

33 maize and its propensity to contaminate grain with toxic compounds. Some isolates of the

34 fungus harbor a meiotic drive element known as *Spore killer* (Sk^K) that causes nearly all

35 surviving meiotic progeny from an $Sk^K \times$ *Spore killer*-susceptible (Sk^S) cross to inherit the Sk^K

36 allele. Sk^K has been mapped to chromosome V but the genetic element responsible for meiotic

37 drive and spore killing has yet to be identified. In this study, we used cleaved amplified

38 polymorphic sequence markers to genotype individual progeny from an $Sk^K \times Sk^S$ mapping

39 population. We also sequenced the genomes of three progeny from the mapping population to

40 determine their single nucleotide polymorphisms. These techniques allowed us to refine the

41 location of Sk^K to a contiguous 102-kb region of chromosome V, herein referred to as the *Sk*

42 locus. Relative to Sk^S genotypes, Sk^K genotypes have one extra gene within this locus for a total

43 of 42 genes. The additional gene in Sk^K genotypes, named *SKL1* for *Spore Killer Locus 1,* is the

44 most highly expressed gene from the *Sk* locus during early stages of sexual development. The *Sk*

45 locus also has three hypervariable regions, the longest of which includes *SKL1*. The possibility

46 that *SKL1,* or another gene from the *Sk* locus, is an essential component of meiotic drive and

47 spore killing is discussed.

48

49   **INTRODUCTION**

50   *Fusarium verticillioides* is an ascomycete fungus that can exhibit both endophytic and

51   pathogenic growth on maize (Bacon and Hinton 1996; White 1998). The fungus is of agriculture

52   concern because of its ability to cause maize ear and stalk rot, and also because it can

53   contaminate maize kernels with a group of mycotoxins known as fumonisins (Marasas 2001;

54   Brown and Proctor 2016). The problems caused by *F. verticillioides* and its myoctoxins were

55   noticed as early as 1970, when the fungus was correlated with an outbreak of Equine

56   Leukoencephalomalacia (ELEM) in South Africa (Kellerman *et al.* 1972). Since then,

57   fumonisins have been confirmed to cause ELEM in horses (Marasas *et al.* 1988; Kellerman *et al.*

58   1990), pulmonary edema in pigs (Harrison *et al.* 1990), and liver cancer in laboratory rats

59   (Gelderblom *et al.* 1988, 1991). Fumonisin-contaminated grain has also been linked to neural

60   tube defects in humans (Missmer *et al.* 2006). Thus, the potential presence of fumonisins, even

61   in apparently healthy grain, makes it necessary to aggressively screen grain for these mycotoxins

62   before it is used in food or feed. Contaminated grain must be destroyed, resulting in crop losses

63   worth millions of dollars per year (Wu, 2007).

64

65   The primary sources of inoculum for endophytic and pathogenic growth of *F.*

66   *verticillioides* on maize are asexual spores, such as macroconidia and microconidia (Munkvold

67   2003). Sexual spores, called ascospores, may also be important to the *F. verticillioides* life cycle

68   (Reynoso *et al.* 2009). Sexual reproduction in this heterothallic fungus begins when the

69   immature fruiting bodies of one strain are fertilized by a strain of opposite mating type (Martin *et*

70   *al.* 2011). Fruiting bodies are called perithecia and meiosis occurs in spore sacs, called asci,

71   within the perithecia. At the start of meiosis, a single diploid nucleus is formed from the haploid

72   genomes of both parents. This diploid nucleus separates into four haploid nuclei through the

73   standard reductional and equational division stages of meiosis, and subsequently, each of these

74   four haploid nuclei undergo a post-meiotic mitosis to form eight nuclei. Each nucleus is then

75   incorporated into a separate ascospore through a process known as ascospore delimitation. A

76   phenotypically normal ascus should thus contain eight ascospores at maturity in *F.*

77   *verticillioides*.

78

79   During normal development, asci break down and ascospores are exuded from perithecia

80   in gelatinous masses. However, it is possible to examine ascospores within intact asci by

81   perithecial dissection. Kathariou and Spieth used this procedure to discover an allele named

82   *Spore killer* (Sk^K). In $Sk^K \times Sk^S$ crosses, where the latter stands for *Spore killer*-susceptible, asci

83   contain four instead of eight ascospores (Kathariou and Spieth 1982). Early stages of ascus

84   development are cytologically-normal in these crosses, but four ascospores degenerate shortly

85   after ascospore delimitation (Raju 1994). The four surviving ascospores are almost always of the

86   Sk^K genotype (Kathariou and Spieth 1982; Xu and Leslie 1996). Unlike $Sk^K \times Sk^S$ crosses, $Sk^K \times$

87   Sk^K crosses produce asci with eight ascospores (Kathariou and Spieth 1982). Thus, the Sk^K allele

88   is sufficient for spore killing and resistance to spore killing.

89

90   The ability of Sk^K-ascospores to kill Sk^S-ascospores suggests that Sk^K could be the

91   predominant allele in some *F. verticillioides* populations. Although the literature is limited on

92   this subject, a screen of 225 *F. verticillioides* isolates from 24 fields across Europe and North

93   America found the Sk^K allele to be present in 81% of isolates (Kathariou and Spieth 1982).

94   Shortly after the discovery of Sk^K in *F. verticillioides*, a spore killing allele was also discovered

95   in *F. subglutinans*. This allele was also named *Spore killer*, but it was given the slightly different

96   notation of SK^k. Along with the report of its discovery, Sidhu (1984) presented evidence that the

97   SK^k allele was present in 10 of 15 *F. subglutinans* isolates obtained from a single maize field.

98   Therefore, Sk^K and SK^k appear to be the predominant alleles in at least some populations of *F.*

99   *verticillioides* and *F. subglutinans*.

100

101   The relationship between Sk^K and SK^k is still unclear despite both being discovered more

102   than 30 years ago. To our knowledge, the only other significant research involving either allele

103   was performed by Xu and Leslie (1996) during construction of a genetic map for *F.*

104   *verticillioides*. During this study, Sk^K was mapped between two restriction fragment length

105   polymorphism (RFLP) markers on chromosome V. These markers, named RFLP1 and 11p18,

106   are located 2.5 cM and 8.6 cM from Sk^K, respectively (Xu and Leslie 1996). Xu and Leslie's

107   mapping population was derived from an $Sk^K \times Sk^S$ cross, and interestingly, only one progeny

108   from over 100 did not inherit the Sk^K allele (Xu and Leslie 1996). This evidence demonstrates

109   that Sk^K can achieve transmission rates of over 99 percent in laboratory crosses.

110

111   An *F. verticillioides* reference genome, derived from an Sk^S strain known as Fv149-Sk^S,

112   was published 14 years after the initial mapping of Sk^K (Ma *et al.* 2010). Here, we advance

113   *Fusarium* Spore killer research by delineating physical borders for Sk^K with respect to the *F.*

114   *verticillioides* reference genome. Our data place Sk^K within a 102-kb contiguous sequence of

115   DNA, which we refer to as the *Sk* locus. Notable differences exist between the *Sk* locus in

116   Fv999-Sk^K and Fv149-Sk^S strains. These are described and discussed below.

117

6

118 **MATERIAL AND METHODS**

119 **Strains, media and culture conditions**

120 Key strains are listed in Table 1. Vegetative propagation was performed on V8 Juice Agar

121 (VJA) (Tuite, 1969) in 16 mm test tubes at room temperature on a laboratory benchtop. Carrot

122 agar (CA), which was originally described by Klittich and Leslie (1988), was prepared as

123 follows: 200 g of organic peeled baby cut carrots were autoclaved in 200 ml of water, pureed

124 with a blender, then adjusted to 500 ml with sterile water to create a 1× stock. Diluted CA (*e.g.*,

125 0.1× and 0.25×) was prepared by mixing the appropriate volumes of 1× CA stock and sterile

126 water, before adding agar to a final concentration of 2% and autoclaving. Liquid Vogel's

127 Minimal Medium (VMM, Vogel 1956) or GYP medium (2% glucose, 1% peptone, and 0.3%

128 yeast extract) were used to produce mycelia for genomic DNA isolation. Liquid cultures for

129 genomic DNA isolation were incubated at 28 ºC in the dark without agitation.

130

131 **Sexual crosses**

132 Crosses were performed on CA in a similar manner to previously described methods (Klittich

133 and Leslie 1988). Asexual spores (conidia) from the female parent were transferred to the center

134 of a 60 mm petri dish containing 20 ml of CA or diluted CA. The female parent was then

135 cultured for 10-14 days before fertilization with a suspension of conidia from the male parent.

136 Conidial suspensions were prepared by adding 2.0 ml of 0.001% Tween-20 to a 10-14 day old

137 test-tube culture of the male parent and dislodging the conidia with a pipette tip. Fertilization

138 was performed by transferring 1.0 ml of a conidial suspension of the male parent to the surface

139 of a culture of the female parent. The conidial suspension was spread over the surface of the

140 female culture with a glass rod. Crosses were incubated in a culture chamber that alternated

7

141   between 23.0 ºC (12 hours, light) and 22.5 ºC (12 hours, dark). Light was provided by white

142   (Philips F34T12/CW/RS/EW/ALTO) and black (General Electric F40T12BL) fluorescent lamps.

143

144   The Fv999-Sk^K × Fv149-Sk^S mapping population

145   In *F. verticillioides*, ascospores are exuded from mature perithecia in a hair-like structure called a

146   cirrus. To obtain an Sk^K mapping population, Fv999-Sk^K was crossed with Fv149-Sk^S and cirri

147   were isolated from the tops of a few perithecia with a sterile needle, dispersed in sterile water,

148   and spread onto a plate of 4% water agar. Germinating ascospores were transferred to VJA in 16

149   mm test tubes.

150

151   Microscopy

152   Asci were dissected from perithecia in 25% glycerol under magnification. A Vanguard 1433Phi

153   light microscope and attached digital camera (Amscope MU1000) were used for imaging. The

154   condenser and aperture diaphragm were set for high contrast, which allowed for the number of

155   ascospores in mature asci to be determined without tissue staining.

156

157   DNA methods

158   Genomic DNA was prepared using one of three methods. In method one, strains were cultured

159   in 25 ml liquid VMM at 28 °C in the dark for three days. Mycelia were washed with 0.9% NaCl

160   and dried by lyophilization before extraction with IBI Scientific's Genomic DNA Mini Kit for

161   Plants. Method two, based on Henderson *et al.* (2005), was used as an inexpensive and time-

162   efficient alternative to method one. A 6" plain-tipped wood applicator was used to transfer ≤ 10

163   mg of conidia to 200 µl of TE buffer (10 mM Tris, 1 mM EDTA, pH 8.0). The suspension was

8

164   boiled at 105 °C in a heat block for 12 minutes, incubated on ice for 2 minutes, then vortexed for

165   5 seconds. Insoluble material was pelleted at 15,000 × g for 10 minutes at room temperature,

166   after which 25 μl of supernatant was transferred to a new vial and frozen at -20 °C for storage.

167   In our hands, this method works well for the amplification of PCR products shorter than 1 kb.

168   Method three was used for the preparation of genomic DNA for high-throughput sequencing.

169   Strains were cultured in 25 ml of liquid GYP at 28 °C for 48 hrs. Mycelia was washed with

170   water and DNA was extracted with the Zymo Research Fungal DNA Miniprep Kit.

171

172   Polymerase chain reaction (PCR) assays were performed with MidSci Bullseye Taq DNA

173   Polymerase or New England Biolabs Phusion High-Fidelity DNA Polymerase.

174

175   **Genome sequencing**

176   DNA libraries for MiSeq sequencing (Illumina) were constructed from 1 ng of genomic DNA

177   using the Illumina Nextera XT DNA Library Preparation Kit. Sequencing was performed with

178   MiSeq Reagent Kit Version 3. Adapters were removed and low-quality reads were trimmed with

179   CLC Genomics Workbench (Version 8.0). The datasets were deposited in the National Center

180   for Biotechnology Information's (NCBI) Sequence Read Archive (Leinonen *et al.* 2011). They

181   can be obtained with the following accession numbers: SRR3271586 (Fv999-Sk^K), SRR3273544

182   (JP98.75-Sk^K), SRR3273545 (JP98.111-Sk^K), and SRR3273546 (JP98.118-Sk^K). The data sets

183   are of high-quality. For example, draft genomes were assembled with CLC Genomics

184   Workbench and all assemblies had N50 values over 90 kb with coverage levels between 49 and

185   73 fold (Table 2).

186

9

CAPS markers

Cleaved amplified polymorphic sequence (CAPS) markers (Konieczny and Ausubel 1993) were used to help refine the location of Sk^K (Table 3). CAPS markers were identified by first aligning genome sequencing reads from strain Fv999-Sk^K to the Fv149-Sk^S reference genome (NCBI, ASM14955v1) and then visually scanning aligned reads with Tablet (Milne *et al.* 2010) for polymorphisms in GGCC sites. This four-base sequence is cleaved by the restriction endonuclease *Hae*III. Six CAPS markers on chromosome V were chosen for this study, along with one CAPS marker on each of chromosomes I, VII, and XI (Table 3). PCR-primers for each CAPS marker were designed to amplify a short product (< 500 bp) from both Fv999-Sk^K and Fv149-Sk^S sequences. The PCR primers used for amplification of each CAPS marker are described in Table S1.

The following protocol was used to analyze the segregation patterns of CAPS markers in each individual of the Fv999-Sk^K × Fv149-Sk^S mapping population. Genomic DNA was isolated from each progeny, CAPS markers were amplified by PCR, and PCR products were digested with *Hae*III. The digested products were then examined for Fv999-Sk^K or Fv149-Sk^S cleavage patterns by gel electrophoresis on standard 1% agarose-TAE (40mM Tris, 20mM acetic acid, and 1mM EDTA) gels. The *Hae*III-based DNA digest patterns of each CAPS marker for Fv999-Sk^K and Fv149-Sk^S alleles are listed in Table S2.

Single nucleotide polymorphisms (SNPs)

10

209   Reads from each MiSeq dataset were aligned to the reference genome of strain Fv149-Sk^S with

210   Bowtie 2 (Langmead and Salzberg 2012). SAMtools 1.3 and BCFtools 1.3 were then used to

211   report SNPs in variant call format (VCF) (Li *et al.* 2009; Danecek *et al.* 2011). Only reads that

212   matched to a single region of Fv149-Sk^S with less than 10 mismatches were used to produce the

213   VCF files. Custom Perl scripts were then used to extract significant SNPs from the VCF files.

214   Significant SNPs were defined as those which were supported by at least 90% of reads at each

215   position. Only positions covered by more than nine reads were considered. Polymorphisms

216   caused by insertions or deletions were ignored.

217

218   **Gene predictions**

219   Protein-coding genes within the *Sk* locus of Fv999-Sk^K were predicted as follows: first, the

220   sequence of the *Sk* locus in Fv999-Sk^K was obtained by *de novo* assembly of MiSeq reads (Table

221   2); second, the coding sequences of annotated genes from the *Sk* locus of Fv149-Sk^S were

222   obtained from GenBank (CM000582.1); third, the Fv149-Sk^S coding sequences were aligned to

223   the *Sk* locus of Fv999-Sk^K with Clustal Omega (Sievers *et al.* 2011; Li *et al.* 2015); and fourth,

224   the alignments were used to manually annotate protein-coding sequences within the sequence of

225   the Fv999-Sk^K *Sk* locus. These steps identified 41 putative protein-coding genes within the *Sk*

226   locus of Fv999-Sk^K. Augustus 3.2.1 (Stanke and Waack 2003) was then used for *de novo*

227   prediction of protein-coding genes. Augustus predictions matched our manual annotation with

228   the notable exception of an additional identified gene (*SKL1*, described below) within the *Sk*

229   locus of Fv999-Sk^K. The complete sequence and annotation of the 102-kb Sk^K locus from Fv999-

230   Sk^K can be obtained from GenBank with accession number KU963213.

231

232   **RESULTS**

233   **Increased production of fruiting bodies by strain Fv999-Sk^K on diluted CA**

234   Directional crosses are often used to investigate sexual processes in heterothallic ascomycete

235   fungi. In this type of cross, one parent is designated as the female and the other is designated as

236   the male. The female provides protoperithecia, *i.e.*, immature fruiting bodies, which are

237   fertilized by conidia from the male. After fertilization, protoperithecia develop into perithecia.

238   　　　　Carrot Agar (CA) is commonly used as a growth medium to study sexual processes in *F.*

239   *verticillioides*. Its preparation essentially involves purchasing carrots from a local market,

240   followed by peeling, blending, and autoclaving a predetermined weight of carrots within a

241   specified volume of water (Leslie and Summerell 2006). Because we were curious about how

242   the amount of carrot in CA medium influences the productivity of Fv999-Sk^K × Fv149-Sk^S

243   crosses, Fv999-Sk^K was cultured on 0.001×, 0.01×, 0.1×, 0.25×, 0.5×, and 1.0× CA, then

244   fertilized with Fv149-Sk^S conidia. The crosses performed on 0.1× and 0.25× CA resulted in

245   nearly three to six fold more perithecia than the crosses performed on 0.5× and 1.0× CA (Figure

246   1). No perithecia were produced when crosses were performed on 0.001× and 0.01× CA (Figure

247   1). Additionally, less conidia were produced on 0.1× CA than on 0.25× CA (data not shown).

248   Because conidia can be a source of cross-contamination, 0.1× CA was used as the crossing

249   medium for the remainder of this study.

250

251   **RFLP 11p18 overlaps with *FVEG_02851* on chromosome V**

252   Although the sequence of RFLP1 was not available, we obtained the sequence of RFLP 11p18

253   from the *Fusarium* Comparative Database. We used this sequence as the query in a BLASTn

254   (Altschul *et al.* 1990) search of the *F. verticillioides* reference genome. This search identified

12

255   positions 1672753 to 1673602 on chromosome V (CM000582.1) as a match to 11p18. This

256   region overlaps with most of the predicted coding sequence of gene *FVEG_02851*, which spans

257   positions 1672886 to 1673769 and encodes a protein of unknown function. Its position on

258   chromosome V was used to choose CAPS markers near the *Sk* locus (Figure 2A).

259

260   **Loci linked to Sk^K drive through meiosis**

261   To begin refining the location of Sk^K on chromosome V, Fv999-Sk^K was crossed with Fv149-Sk^S

262   and the segregation patterns of nine CAPS markers were examined in 60 progeny. Both Fv999-

263   Sk^K and Fv149-Sk^S patterns were inherited in a 1:1 ratio for chromosomes XI, VII, and I. In

264   contrast, Fv999-Sk^K patterns of CAPS markers on chromosome V were inherited more frequently

265   (>= 79.6%) than expected (Figure 2B and Table S3). The only exception was CAPS-5, which is

266   located approximately 20 kb from a telomere (Figure 2A and Table 3). Overall, these results

267   mark the first independent confirmation of Xu and Leslie's (1996) original findings on the biased

268   recovery of molecular markers linked to Sk^K in $Sk^K \times Sk^S$ crosses.

269

270   **Genome sequencing refines the *Sk* locus to a 102-kb region of chromosome V.**

271   To delineate the position of Sk^K on chromosome V, we narrowed our focus to progeny JP98.75-

272   Sk^K, JP98.111-Sk^K, and JP98.118-Sk^K. Even though CAPS marker analysis failed to identify an

273   Fv999-Sk^K region of chromosome V that was inherited by all three progeny (Figure 2C, black

274   shaded regions), all were determined to carry the Sk^K allele by phenotypic analysis (Figure 3 and

275   data not shown). Therefore, their genomes were sequenced (Table 2) and their SNPs along

276   chromosome V were examined. This analysis allowed us to identify two additional

277   recombination events. Both of these recombination events occurred between CAPS markers

13

278   CAPS-3 and CAPS-4 in the ascus producing progeny JP98.111-Sk^K (Figure 2D), explaining why

279   they were not revealed by our CAPS marker analysis. More importantly, the SNP profiles of all

280   three progeny require that Sk^K be located between positions 665,669 and 767,411 (Figure 2D, red

281   lines) with respect to the reference sequence (GenBank, CM000582.1). We refer to this 102-kb

282   contiguous sequence as the *Sk* locus (GenBank, KU963213).

283

284   **Sk^K strains carry a unique gene in the *Sk* locus**

285   The *Sk* locus spans 102,256 bases in Fv999-Sk^K, but only 101,743 bases in Fv149-Sk^S. A

286   ClustalW-based alignment (Thompson *et al.* 1994) of the sequences from both strains is 102,557

287   bases long, with 301 gaps in the Fv999-Sk^K sequence and 814 gaps in the Fv149-Sk^S sequence

288   (Figure 4). To identify specific regions in Sk^K and Sk^S strains with high levels of SNPs or gaps,

289   the number of SNPs or gaps were calculated for each 100-base window across the alignment. A

290   qualitative analysis of these results finds at least three hypervariable regions (Figure 4). One of

291   the shorter hypervariable regions spans genes *FVEG_03180* to *FVEG_03175*, while another

292   spans genes *FVEG_03174* and *FVEG_03173* (Figure 4). The longest hypervariable region is

293   approximately 14 kb long, spans gene FVEG_03167, and extends to the right border of the *Sk*

294   locus (Figure 4).

295

296   The 102-kb *Sk* locus in strain Fv149-Sk^S includes 41 putative protein coding genes

297   (Figure 4 and Table 4). The *Sk* locus in Fv999-Sk^K carries the same 41 genes as well as one

298   additional protein coding gene, *SKL1* (for *Spore Killer Locus 1*), that is located between

299   *FVEG_03165* and *FVEG_03164* (Figure 4). . BLASTp analysis (Altschul *et al.* 1997) of the

300   NCBI non-redundant protein database with the predicted 70-amino acid sequence of the putative

14

301   Skl1 protein identified hypothetical proteins with Expect values ranging from 2×10^{-49} to 8×10^{-04}

302   from various *formae speciales* of the *F. oxysporum* species complex. No significant hits were

303   identified in other species (data not shown). A search of the NCBI Conserved Domain Database

304   (Marchler-Bauer *et al.* 2010) failed to identify a domain within Skl1.

305

306   To confirm that *SKL1* is absent in Fv149-Sk^S, the sequences corresponding to the

307   *FVEG_03165-FVEG_03164* intergenic region from Fv999-Sk^K and Fv149-Sk^S were aligned and

308   examined. This intergenic region consists of 1,234 and 755 bases in Fv999-Sk^K and Fv149-Sk^S

309   respectively (Figure S1). Examination of the alignment revealed that this difference in length

310   was due to the presence of *SKL1* in Fv999-Sk^K and its absence in Fv149-Sk^S (Figure S1). To

311   confirm that the absence of *SKL1* in Fv149-Sk^S was not due to an error in the reference genome

312   sequence, we examined the lengths of the *FVEG_03165-FVEG_03164* intergenic region by PCR

313   in our laboratory stocks of Fv999-Sk^K and Fv149-Sk^S. The PCR product lengths were consistent

314   with the presence of *SKL1* in Fv999-Sk^K and its absence in Fv149-Sk^S (Figure 5).

315

316   ClustalW alignments were used to investigate the level of polymorphism between

317   proteins encoded by the *Sk* locus in Fv999-Sk^K and Fv149-Sk^S strains (Table 4). Analysis of

318   these pairwise alignments revealed that Fveg_15199 is the most polymorphic protein of the

319   locus. Only 80% of the 133 amino acids of Fveg_15199 are identical between the two strains.

320   This is a remarkably high level of polymorphism given that 34 of the 41 shared proteins within

321   the *Sk* locus of Fv999-Sk^K and Fv149-Sk^S are greater than 94% identical, and 40 of 41 are greater

322   than 88% identical (Table 4). A BLASTp search of the NCBI non-redundant protein database

323   identified homologs of Fveg_15199 in several *Fusarium, Neonectria*, *Neosartorya*, and

15

324   *Aspergillus* species, among others (data not shown). A search of the NCBI Conserved Domain

325   Database failed to identify a domain within Fveg_15199.

326

327   To shed light upon the transcriptional profile of protein-coding genes within the *Sk* locus,

328   we analyzed five *F. verticillioides* RNAseq datasets from NCBI's Sequence Read Archive.

329   These datasets were for five time points following the induction of sexual development in a cross

330   of Fv999-*Sk^K* × Fv149-*Sk^S* (Sikhakolli *et al.* 2012). Of the genes within the *Sk* locus,

331   *FVEG_03171* exhibited the greatest increase in expression from the first to last time point (Table

332   5), suggesting that this gene may have an important role during later stages of sexual

333   development. The corresponding protein, Fveg_03171, includes a WSC-domain (data not

334   shown), which has been linked to carbohydrate-binding, cell wall integrity, and stress response.

335   The gene *FVEG_03194* exhibited the greatest fold change over all five time points (>1050×)

336   (Table 5). The Fveg_03194 protein does not have any recognized domains, although it is

337   conserved in *Fusarium*, *Nectria*, *Trichoderma*, *Colletotrichum,* and a few other fungi (data not

338   shown). Interestingly, *SKL1* reached the highest level of expression of all examined genes 2

339   hours after fertilization (Table 5). Furthermore, *SKL1* transcript levels were second only to

340   *FVEG_03197* at the last time point (144 h, Table 5). The latter gene appears to be widely

341   conserved among bacteria and eukaryotes (data not shown), but a function for it or its homologs

342   is unknown.

343

16

344   **DISCUSSION**

345   The segregation of alternate alleles into separate gametes during meiosis encourages genetic

346   conflict (Burt and Trivers 2008). Evidence for this is found in meiotic drive, which occurs when

347   an allele is transmitted through meiosis in a biased manner. Meiotic drive elements are found in

348   a diverse range of fungi, where they achieve biased transmission through sexual reproduction by

349   killing meiospores carrying an alternate allele (Turner and Perkins 1979; Kathariou and Spieth

350   1982; Raju 1994; Dalstra *et al.* 2003; Grognet *et al.* 2014). Thus, fungal meiotic drive elements

351   are often referred to as Spore killers. The molecular basis of meiotic drive by most Spore killers

352   is unknown.

353

354   The existence of meiotic drive by spore killing in *Fusarium* was first recognized in 1982.

355   More than three decades later, we still do not understand the molecular mechanism that mediates

356   this process. This is similar to the situation in *Neurospora*, where three distinct spore killers,

357   known as *Sk-1*, *Sk-2*, and *Sk-3*, were identified in 1979 (Turner and Perkins 1979). A

358   breakthrough in *Sk-2* research was recently made by refining the location of an *Sk-2* resistance

359   gene to a 52-kb sequence of DNA (Hammond, Rehard, Harris, *et al.* 2012). This provided the

360   necessary foundation to clone and characterize the *Sk-2* resistance gene (Hammond, Rehard,

361   Xiao, *et al.* 2012), which, in turn, allowed for the isolation of killer-less *Sk-2* mutants (Harvey *et*

362   *al.* 2014). Here, we have taken a similar approach towards identifying the genetic basis for Sk^K

363   in *F. verticillioides* by first refining the position of Sk^K to a 102-kb region of chromosome V.

364

365   As with previous work on Sk^K (Xu and Leslie 1996), we observed a biased transmission

366   of Sk^K-linked molecular markers (Figure 2B). This is not unexpected since the driving ability of

17

367   Sk^K should also affect the transmission of alleles linked to Sk^K. This phenomenon is referred to

368   as genetic hitchhiking (Lyttle 1991). The closer a hitchhiker is to a meiotic driver, the more

369   likely it is to be transmitted to the next generation through the sexual cycle. In our study,

370   patterns of CAPS markers from the parent Fv999-Sk^K were inherited at a higher frequency than

371   could be attributed to chance alone for five of six markers on chromosome V, and the

372   transmission bias generally decreased with increasing distance from the Sk locus (Figure 2B).

373   Surprisingly, CAPS-1 and CAPS-2 demonstrated higher levels of hitchhiking than CAPS-4

374   (Figure 2B), despite the latter being closer to the Sk locus (Figure 2D). One explanation for this

375   could be the existence of a recombination hotspot between CAPS-4 and the Sk locus; however,

376   we do not have additional data to support this hypothesis.

377

378   While a recombination hotspot could explain the unexpected decrease in hitchhiking for

379   CAPS-4, the opposite phenomenon of recombination-suppression is often associated with

380   meiotic drive elements (reviewed by Lyttle 1991). For example, *Neurospora Sk-2* requires

381   specific alleles of at least two genes to mediate drive, a resistance gene called *rsk* and a killer

382   gene called *rfk* (Hammond, Rehard, Xiao, *et al.* 2012; Harvey *et al.* 2014). Each gene is located

383   on a different arm of chromosome III (Harvey *et al.* 2014). For *Sk-2* to succeed as a meiotic

384   driver, it is imperative that an *Sk-2* ascospore inherit both *rsk* and *rfk* alleles because loss of *rsk*

385   from *Sk-2* leads to a self-killing genotype (Hammond, Rehard, Xiao, *et al.* 2012). This helps

386   explain why *Sk-2* is associated with a 30 cM long "recombination-blocked" region of

387   chromosome III (Campbell and Turner 1987; Harvey *et al.* 2014). By suppressing

388   recombination between *rsk* and *rfk*, *Sk-2* prevents these critical components of its meiotic drive

389   mechanism from separating during meiosis. With respect to *F. verticillioides* Sk^K, recombination

390   suppression, if it exists at all, does not appear to be a significant phenomenon. For example, our

391   CAPS marker analysis identified twelve recombination events between CAPS-3 and CAPS-4 (n

392   = 59, Table S3), and two recombination events between CAPS-2 and CAPS-3 (n = 59, Table

393   S3). This relatively high number of recombination events near the *Sk* locus argues against an *Sk-*

394   *2*-like recombination block for Sk^K.

395

396   If *F. verticillioides* Sk^K requires multiple genes to function as a meiotic drive element, all

397   should be found within the 102-kb *Sk* locus defined by this study. For example, SNP-profiling of

398   progeny JP98.75-Sk^K, JP98.111-Sk^K, and JP98.118-Sk^K indicated that only this region of

399   chromosome V is common between them and the Fv999-Sk^k parent (Figures 2D and Figure 4).

400   Assuming spore killing is mediated by two or more distinct genes within the *Sk* locus, the close

401   proximity of these alleles may negate the requirement for a *Neurospora Sk-2*-like recombination

402   block. Alternatively, meiotic drive and spore killing may be mediated by a single gene. A fungal

403   precedent for this is seen in the *het-s* spore killing mechanism of *Podospora anserina* (Coustou

404   *et al.* 1997; Saupe 2011). This system is controlled by two alternate alleles of a single gene,

405   named *het-s* and *het-S*. The former, *het-s,* encodes the HET-s prion and is the meiotic driver,

406   while the latter, *het-S,* encodes the HET-S protein. Interaction of the HET-s prion with HET-S

407   causes HET-S to relocate to cell membranes, resulting in cell death, presumably through loss of

408   membrane integrity (Seuring *et al.* 2012). The *het-s* ascospores escape cell death because they

409   do not produce the HET-S protein, and thus the *het-s* prion is not toxic to them. This is one

410   example of how meiotic drive and spore killing can be mediated by alternate alleles of a single

411   gene in fungi. Grognet *et al.* (2014) have recently identified *spok1* and *spok2*, two additional

19

412   spore killing genes in *P. anserina,* both of which appear to be single-gene-based meiotic drive

413   systems.

414

415   In the current study, comparative sequence analysis revealed multiple differences

416   between the 102-kb *Sk* locus from Sk^K and Sk^S strains of *F. verticillioides.* Presumably, one or

417   more of these differences is the genetic basis for the different *Sk* phenotypes exhibited by the

418   strains. An analysis of SNPs and gaps identified at least three hypervariable regions within the

419   locus (Figure 4). The interspersed nature of these regions is somewhat surprising and suggests

420   that they could be under the influence of different selective pressures than the less variable

421   regions of the *Sk* locus. The most striking difference between the *Sk* locus is the presence the

422   *SKL1* gene in Sk^K strains and its absence in Sk^S strains. Differences between the hypervariable

423   regions and *SKL1* in Sk^K versus Sk^S strains raise at least two key questions: 1) are the

424   hypervariable regions and/or *SKL1* responsible for spore killing, and 2) do they correspond to the

425   Sk^K allele that was previously defined by phenotypic analysis (Kathariou and Spieth 1982). The

426   high levels of expression of *SKL1* throughout sexual development are consistent with its

427   involvement in sexual reproduction. However, in addition to *SKL1* and the hypervariable

428   regions, there are also numerous less dramatic sequence differences between genes and

429   intergenic regions of the *Sk* locus in Sk^K and Sk^S strains. The current data does not rule out the

430   possibility that one or more of these differences is responsible for the Sk^K and Sk^S phenotypes.

431   As a result, our efforts are now focused on targeted deletions of *SKL1* and other regions of the *Sk*

432   locus to determine the genetic basis of the spore killing phenotype in *F. verticillioides.*

433

434

435 **ACKNOWLEDGEMENTS**

448

449 **LITERATURE CITED**

450 Altschul, S.F., W. Gish, W. Miller, E.W. Myers, and D.J. Lipman, 1990   Basic local alignment

451   search tool. J. Mol. Biol. 215: 403–410.

452 Altschul, S. F., T. L. Madden, A. A. Schäffer, J. Zhang, Z. Zhang *et al.*, 1997   Gapped BLAST

453   and PSI-BLAST: a new generation of protein database search programs. Nucleic Acids

454   Res. 25: 3389–3402.

455 Bacon, C. W., and D. M. Hinton, 1996   Symptomless endophytic colonization of maize by

456   *Fusarium moniliforme*. Can. J. Bot. 74: 1195–1202.

457 Brown, D. W., and R. H. Proctor, 2016   Insights into natural products biosynthesis from analysis

458   of 490 polyketide synthases from *Fusarium*. Fungal Genet. Biol. 89: 37-51.

459 Burt, A., and R. Trivers, 2008   *Genes in Conflict: The Biology of Selfish Genetic Elements*.

460   Harvard University Press.

461 Campbell, J. L., and B. C. Turner, 1987   Recombination block in the *Spore killer* region of

462   *Neurospora*. Genome 29: 129–135.

463 Coustou, V., C. Deleu, S. Saupe, and J. Begueret, 1997   The protein product of the *het-s*

464   heterokaryon incompatibility gene of the fungus *Podospora anserina* behaves as a prion

465   analog. Proc. Natl. Acad. Sci. U. S. A. 94: 9773–9778.

466 Dalstra, H.J.P., K. Swart, A.J.M. Debets, S.J. Saupe, and R.F. Hoekstra, 2003   Sexual

467   transmission of the [Het-S] prion leads to meiotic drive in *Podospora anserina*. Proc.

468   Natl. Acad. Sci. U. S. A. 100: 6616–6621.

469 Danecek, P., A. Auton, G. Abecasis, C.A. Albers, E. Banks *et al.*, 2011   The variant call format

470   and VCFtools. Bioinformatics 27: 2156–2158.

471   Gelderblom, W. C., K. Jaskiewicz, W. F. Marasas, P. G. Thiel, R. M. Horak *et al.*, 1988

472   Fumonisins--novel mycotoxins with cancer-promoting activity produced by *Fusarium*

473   *moniliforme*. Appl. Environ. Microbiol. 54: 1806–1811.

474   Gelderblom, W. C., N. P. Kriek, W. F. Marasas, and P. G. Thiel, 1991   Toxicity and

475   carcinogenicity of the *Fusarium moniliforme* metabolite, fumonisin B1, in rats.

476   Carcinogenesis 12: 1247–1251.

477   Grognet, P., H. Lalucque, F. Malagnac, and P. Silar, 2014   Genes that bias Mendelian

478   segregation. PLoS Genet. 10: e1004387.

479   Hall, T. A., 1999   BioEdit: a user-friendly biological sequence alignment editor and analysis

480   program for Windows 95/98/NT. Nucleic Acids Symp. Ser. 41: 95–98.

481   Hammond, T. M., D. G. Rehard, B. C. Harris, and P. K. T. Shiu, 2012   Fine-scale mapping in

482   *Neurospora crassa* by using genome-wide knockout strains. Mycologia 104: 321–323.

483   Hammond, T.M., D.G. Rehard, H. Xiao, and P.K.T. Shiu, 2012   Molecular dissection of the

484   *Neurospora* Spore killer elements. Proc. Natl. Acad. Sci. U. S. A. 109: 12093–12098.

485   Harrison, L. R., B. M. Colvin, J. T. Greene, L. E. Newman, and J. R. Cole Jr., 1990   Pulmonary

486   edema and hydrothorax in swine produced by fumonisin B1, a toxic metabolite of

487   *Fusarium moniliforme*. J. Vet. Diagn. Investig. 2: 217–221.

488   Harvey, A.M., D.G. Rehard, K.M. Groskreutz, D.R. Kuntz, K.J. Sharp *et al.*, 2014   A critical

489   component of meiotic drive in *Neurospora* is located near a chromosome rearrangement.

490   Genetics 197:1165-1174.

491   Henderson, S.T., G.A. Eariss, and D. Catcheside, 2005   Reliable PCR amplification from

492   *Neurospora crassa* genomic DNA obtained from conidia. Fungal Genet. Newsl. 52: 24.

493   Kathariou, S., and P.T. Spieth, 1982   Spore Killer Polymorphism in *Fusarium moniliforme*.

494   Genetics 102: 19–24.

495   Kellerman, T. S., W. F. Marasas, J. G. Pienaar, and T. W. Naudé, 1972   A mycotoxicosis of

496   equidae caused by *Fusarium moniliforme* sheldon. A preliminary communication.

497   Onderstepoort J. Vet. Res. 39: 205–208.

498   Kellerman, T. S., W. F. Marasas, P. G. Thiel, W. C. Gelderblom, M. Cawood *et al.*, 1990

499   Leukoencephalomalacia in two horses induced by oral dosing of fumonisin B1.

500   Onderstepoort J. Vet. Res. 57: 269–275.

501   Klittich, C., and J.F. Leslie, 1988   Nitrate reduction mutants of *Fusarium moniliforme*

502   (*Gibberella fujikuroi*). Genetics 118: 417–423.

503   Konieczny, A., and F.M. Ausubel, 1993   A procedure for mapping *Arabidopsis* mutations using

504   co-dominant ecotype-specific PCR-based markers. Plant J. 4: 403–410.

505   Langmead, B., and S.L. Salzberg, 2012   Fast gapped-read alignment with Bowtie 2. Nat.

506   Methods 9: 357–359.

507   Leinonen, R., H. Sugawara, and M. Shumway, 2011   The sequence read archive. Nucleic Acids

508   Res. 39: D19–21.

509   Leslie, J.F., and B.A. Summerell, 2006   The *Fusarium* Laboratory Manual. Blackwell

510   Publishing, Ames, Iowa.

511   Li, W., A. Cowley, M. Uludag, T. Gur, H. McWilliam *et al.*, 2015   The EMBL-EBI

512   bioinformatics web and programmatic tools framework. Nucleic Acids Res. 43: W580–

513   584.

514   Li, H., B. Handsaker, A. Wysoker, T. Fennell, J. Ruan *et al.*, 2009   The Sequence

515   Alignment/Map format and SAMtools. Bioinformatics 25: 2078–2079.

516   Lyttle, T. W., 1991   Segregation distorters. Annu. Rev. Genet. 25: 511–557.

517   Ma, L.J., H.C. van der Does, K.A. Borkovich, J.J. Coleman, M.J. Daboussi *et al.*, 2010

518   Comparative genomics reveals mobile pathogenicity chromosomes in *Fusarium*. Nature

519   464: 367–373.

520   Marasas, W. F. O., 2001   Discovery and occurrence of the fumonisins: a historical perspective.

521   Environ. Health Perspect. 109(Suppl 2): 239-243.

522   Marasas, W. F., T. S. Kellerman, W. C. Gelderblom, J. A. Coetzer, P. G. Thiel *et al.*, 1988

523   Leukoencephalomalacia in a horse induced by fumonisin B1 isolated from *Fusarium*

524   *moniliforme*. Onderstepoort J. Vet. Res. 55: 197–203.

525   Marchler-Bauer, A., S. Lu, J. B. Anderson, F. Chitsaz, M. K. Derbyshire *et al.*, 2010   CDD: a

526   Conserved Domain Database for the functional annotation of proteins. Nucleic Acids

527   Res. 39: D225–D229.

528   Martin, S. H., B. D. Wingfield, M. J. Wingfield, and E. T. Steenkamp, 2011   Structure and

529   evolution of the *Fusarium* mating type locus: new insights from the *Gibberella fujikuroi*

530   complex. Fungal Genet. Biol. 48: 731–740.

531   McCluskey, K., A. Wiest, M. Plamann, 2010   The Fungal Genetics Stock Center: a repository

532   for 50 years of fungal genetics research. J. Biosci. 35: 119–126.

533   Milne, I., M. Bayer, L. Cardle, P. Shaw, G. Stephen *et al.*, 2010   Tablet—next generation

534   sequence assembly visualization. Bioinformatics 26: 401–402.

535   Missmer, S. A., L. Suarez, M. Felkner, E. Wang, A. H. Merrill Jr. *et al.*, 2006   Exposure to

536   fumonisins and the occurrence of neural tube defects along the Texas-Mexico border.

537   Environ. Health Perspect. 114: 237–241.

538 Mortazavi, A., B. A. Williams, K. McCue, L. Schaeffer, and B. Wold, 2008 Mapping and

539   quantifying mammalian transcriptomes by RNA-Seq. Nat. Methods 5: 621–628.

540 Munkvold, G. P., 2003 Epidemiology of Fusarium diseases and their mycotoxins in maize ears,

541   pp. 705–713 in *Epidemiology of Mycotoxin Producing Fungi*, edited by X. Xu, J. A.

542   Bailey, and B. M. Cooke. Springer Netherlands.

543 Raju, N.B., 1994 Ascomycete spore killers: Chromosomal elements that distort genetic ratios

544   among the products of meiosis. Mycologia 86: 461-473.

545 Reynoso, M. M., S. N. Chulze, K. A. Zeller, A. M. Torres, and J. F. Leslie, 2009 Genetic

546   structure of *Fusarium verticillioides* populations isolated from maize in Argentina. Eur. J.

547   Plant Pathol. 123: 207–215.

548 Saupe, S. J., 2011 The [Het-s] prion of *Podospora anserina* and its role in heterokaryon

549   incompatibility. Semin. Cell Dev. Biol. 22: 460–468.

550 Seuring, C., J. Greenwald, C. Wasmer, R. Wepf, S. J. Saupe *et al.*, 2012 The mechanism of

551   toxicity in HET-S/HET-s prion incompatibility. PLoS Biol. 10: e1001451.

552 Sidhu, G. S., 1984 Genetics of *Gibberella fujikuroi* V. *Spore killer* alleles in *G. fujikuroi*. J.

553   Hered. 75: 237–238.

554 Sievers, F., A. Wilm, D. Dineen, T. J. Gibson, K. Karplus *et al.*, 2011 Fast, scalable generation

555   of high-quality protein multiple sequence alignments using Clustal Omega. Mol. Syst.

556   Biol. 7: 539.

557 Sikhakolli, U. R., F. López-Giráldez, N. Li, R. Common, J. P. Townsend *et al.*, 2012

558   Transcriptome analyses during fruiting body formation in *Fusarium graminearum* and

559   *Fusarium verticillioides* reflect species life history and ecology. Fungal Genet. Biol. 49:

560   663–673.

561 Stanke, M., and S. Waack, 2003   Gene prediction with a hidden Markov model and a new intron

562   submodel. Bioinformatics 19(Suppl 2): 215–225.

563 Thompson, J. D., D. G. Higgins, and T. J. Gibson, 1994   CLUSTAL W: improving the

564   sensitivity of progressive multiple sequence alignment through sequence weighting,

565   position-specific gap penalties and weight matrix choice. Nucleic Acids Res. 22: 4673–

566   4680.

567 Tuite, J., 1969.   Plant Pathological Methods: Fungi and Bacteria. Burgess Publishing Company,

568   Minneapolis.

569 Turner, B.C., and D.D. Perkins, 1979   *Spore killer*, a chromosomal factor in *Neurospora* that

570   kills meiotic products not containing it. Genetics 93: 587–606.

571 Vogel, H.J., 1956   A convenient growth medium for *Neurospora* (Medium N). Microb. Genet

572   Bull 13: 42–43.

573 White, D. G. 1998   *Compendium of corn diseases*. APS Press, St. Paul, Minn.

574 Wu, F. 2007   Measuring the economic impacts of *Fusarium* toxins in animal feeds. Animal Feed

575   Sci. Technol. 137: 363-374.

576 Xu, J.R., and J.F. Leslie, 1996   A genetic map of *Gibberella fujikuroi* mating population A

577   (*Fusarium moniliforme*). Genetics 143: 175–189.

578 Xu J.R., K. Yan, M. B. Dickman, and J. F. Leslie, 1995   Electrophoretic karyotypes distinguish

579   the biological species of *Gibberella fujikuroi* (*Fusarium* Section Liseola). Mol. Plant.

580   Microbe Interact. 8: 74–84.

581

582   **Figure and Table Legends**

583   **Figure 1** Perithecial production on different CA media. Cultures of Fv999-Sk^K were grown on

584   CA media containing different concentrations of carrot and fertilized with conidia from strain

585   Fv149-Sk^S. The data represent the total number of perithecia observed 25 days after fertilization.

586   Crosses were performed in triplicate and error bars are standard deviation.

587

588   **Figure 2** The *F. verticillioides Sk* locus is found within a 102-kb region of chromosome V. A)

589   A diagram of the 4.25 Mb sequence of chromosome V from Fv149-Sk^S is shown. The annotated

590   chromosome V sequence was downloaded from NCBI (CM000582.1). The first gene

591   (*FVEG_03430*) and last gene (*FVEG_16592*) on the chromosome are indicated. The location of

592   RFLP marker 11p18 is also shown. Marker 11p18 overlaps gene *FVEG_02851*. B) A total of 60

593   progeny were isolated from a cross between Fv999-Sk^K and Fv149-Sk^S. These progeny were

594   genotyped with nine different CAPS markers. Markers CAPS-1 through CAPS-6 are located on

595   chromosome V. Markers CAPS-9, CAPS-10, and CAPS-11 are found on chromosomes XI, VII,

596   and I, respectively. Each bar represents the percentage of Fv999-Sk^K genotypes recovered for

597   each marker. An asterisk is placed above all markers whose recovery deviated significantly from

598   a Mendelian ratio of 1:1 according to a χ^2 test with $p < 0.01$. The biased transmission of Fv999-

599   Sk^K sequences was detected for all markers on chromosome V, except for CAPS-5. (C) The

600   marker patterns for progeny JP98.75-Sk^K, JP98.111-Sk^K, and JP98.118-Sk^K suggest that crossover

601   events occurred between CAPS-3 and CAPS-4 (for JP98.75-Sk^K), CAPS-4 and CAPS-5 (for

602   JP98.111-Sk^K), and CAPS-2 and CAPS-3 (for JP98.118-Sk^K) (Table S3). These crossovers do

603   not reveal an Fv999-Sk^K-derived chromosome V sequence common to all three progeny. The

604   predicted Fv999-Sk^K- and Fv149-Sk^S-inherited regions are shown in black and white,

28

605   respectively. Irregular borders are used to indicate that the exact crossover positions cannot be

606   determined from the marker data. (D) SNP analysis was used to more accurately define

607   crossover positions for progeny JP98.75-Sk^K, JP98.111-Sk^K, and JP98.118-Sk^K, and to discover

608   additional crossovers. This analysis identified two additional recombination events on

609   chromosome V of JP98.111-Sk^K, which delineate a single contiguous region between 665.7 kb

610   and 767.4 kb on chromosome V as the only Fv999-Sk^K region common to all three progeny (red

611   dotted lines). This region is referred to as the *Sk* locus.

612

613   **Figure 3** Representative images of killing and no-killing in *F. verticillioides* asci. (A) Asci

614   from a cross of progeny JP98.111-Sk^K with BM43.31-Sk^K. Eight ascospores can be detected in

615   most of the mature asci, confirming that progeny JP98.111-Sk^K carries the Sk^K allele. (B) Asci

616   from a cross of progeny JP98.111-Sk^K with Fv149-Sk^S. Only four ascospores are detected in

617   most of the mature asci, again confirming that progeny JP98.111-Sk^K carries the Sk^K allele. The

618   asterisk denotes an ascus where there appears to be five ascospores. Two possible explanations

619   are that this 5th ascospore escaped killing, or, it strayed from another ascus during the dissection

620   and imaging process.

621

622   **Figure 4** Strain Fv999-Sk^K carries a unique gene within a hypervariable region of the *Sk* locus.

623   The *Sk* locus from Fv999-Sk^K (GenBank, KU963213) and Fv149-Sk^S (GenBank, CM000582.1,

624   positions 665,669 to 767,411) were imported into BioEdit (Version 7.2.5) (Hall 1999) and

625   aligned with ClustalW. Custom Perl scripts were used to examine base mismatches, gap

626   positions, and to generate the diagram. The total number of mismatches (SNPs) between the two

627   sequences was calculated for each 100-base, non-overlapping window of the alignment. The

29

628   total number of gaps was also calculated for each 100-base, non-overlapping window. A gap

629   position was not considered an SNP. By this definition, a window with 100 gaps can have no

630   SNPs. Black rectangles represent the coding regions of predicted genes. Gene names are

631   abbreviated according to their identification tags in the Fv149-Sk^S annotation. For example:

632   *FVEG_03199* is shortened to *3199*. A striking feature of the alignment is the presence of at least

633   three hypervariable regions; approximately spanning *FVEG_03180* to *FVEG_03175*,

634   *FVEG_3174* to *FVEG_3173*, and *FVEG_03167* to the right border. A second striking feature is

635   the presence of a unique gene, *SKL1,* in Fv999-Sk^K only.

636

637   **Figure 5** The *Sk* locus in Fv149-Sk^S is missing *SKL1*. To confirm that *SKL1* is missing from the

638   *Sk* locus in Fv149-Sk^S, genomic DNA was isolated from two liquid cultures of Fv149-Sk^S and

639   two liquid cultures of Fv999-Sk^K. All four genomic DNA samples were used as templates in

640   standard PCR reactions with the following oligonucleotide primers: 5'

641   CGAATGACCTGGGGAGCCATAA 3' and 5' TCTCTCCACCACCTCCATCAGC 3', which

642   amplify the *FVEG_03165-FVEG_03164* intergenic regions in Fv999-Sk^K and Fv149-Sk^S. PCR

643   products were visualized by ethidium bromide staining after electrophoresis through a 1%

644   agarose-TAE gel. We observed PCR products with lengths that are consistent with the absence

645   of *SKL1* in Fv149-Sk^S (287 bp) and the presence of *SKL1* in Fv999-Sk^K (767 bp).

646

647   **Figure S1** A ClustalW alignment of the *FVEG_03165-FVEG_03164* intergenic region from

648   Fv999-Sk^K and Fv149-Sk^S. The coding start site of flanking gene *FVEG_03165* is indicated with

649   a blue arrow. Similarly, the coding stop site of flanking gene *FVEG_03164* is indicated with a

30

650   blue line. The predicted coding sequence of *SKL1* is indicated with a red line. This alignment

651   shows that *SKL1* is present in Fv999-Sk^K but not in Fv149-Sk^S.

652

653   **Table 1 Key strains used in this study**

654   [1]Throughout the text, the suffix -Sk^K or -Sk^S is added to each strain name to denote genotype with

655   respect to *Sk*. [2]McCluskey *et al*. 2010; [3]Xu *et al*. 1995; [4]Xu and Leslie 1996.

656

657   **Table 2 Draft genome assembly statistics**

658   [1]total, the total length of each genome assembly; [2]avg. length, the average length of each read in

659   the assembly; [3]coverage, calculated by multiplying the number of reads by the average read

660   length and dividing the product by 41.9 Mb, the genome size of Fv149-Sk^S (NCBI

661   ASM14955v1).

662

663   **Table 3 Marker locations**

664   Marker locations on chromosomes I, V, VII, and XI of *F. verticillioides* Fv149-Sk^S (NCBI

665   ASM14955v1).

666

667

668

669

670

671

672

673

674 **Table 4 Comparison of predicted protein-coding sequences within the *Sk* locus of Fv999-**

675 ***Sk^k* and Fv149-*Sk^S***

676 The sequences of predicted proteins within the *Sk* locus of Fv999-*Sk^K* and Fv149-*Sk^S* were

677 imported into Bioedit 7.2.5 (Hall 1999) and aligned with ClustalW (Thompson *et al.* 1994).

678 Sequence alignments were then analyzed for percent identity and percent similarity. Gapped-

679 positions were excluded from the identity and similarity calculations.

680

681 **Table 5 Expression analysis of genes from the *Sk* locus during sexual development**

682 Sikhakolli *et al.* (2012) analyzed transcriptional changes in *F. verticillioides* during fruiting body

683 development in Fv999-*Sk^K* × Fv149-*Sk^S* crosses by RNA sequencing (RNAseq) and deposited the

684 datasets in NCBI's Sequence Read Archive (Leinonen *et al.* 2011). The following datasets were

685 downloaded from the database: 2 hours post fertilization (hpf) (SRR1592416), 24 hpf

686 (SRR1592417), 48 hpf (SRR1592418), 72 hpf (SRR1592419), 96 hpf (SRR1592420), and 144

687 hpf (SRR1592421). Reads were aligned to coding sequences for the 42 genes (plus flanking

688 genes *FVEG_03199* and *FVEG_03163*) from the *Sk* locus in Fv999-*Sk^K* with Bowtie 2

689 (Langmead and Salzberg 2012). RPKK values, or, reads per kilobase exon model per thousand

690 mapped reads, were calculated for each gene. We then performed the same alignment and RPKK

691 calculation procedure for the coding sequences of the 41 genes from the *Sk* locus (plus flanking

692 genes *FVEG_03199* and *FVEG_03163*) in Fv149-*Sk^S*. The RPKK values in the table are the

693 average of the two RPKK calculations for each gene, except for *SKL1*, which is only found in

694 Fv999-*Sk^K*. RPKK is a variation upon RPKM as described by (Mortazavi *et al.* 2008). [1]The

695 minimum RPKK in the table. [2]The maximum RPKK in the table. [3]Fold change was calculated by

32

696   dividing the maximum RPKK by the minimum RPKK to identify the genes undergoing the

697   greatest expression change during the first 144 hours after fertilization. If the minimum RPKK

698   for a gene was 0, it was arbitrarily assigned a minimum RPKK of 0.1 to approximate a fold

699   change value.

700

701

702   **Table S1 Oligonucleotide primers for CAPS markers**

703

704   **Table S2 CAPS marker sizes**

705

706   **Table S3 Genotypes of the Fv999-Sk^K × Fv149-Sk^S mapping population**

707

708
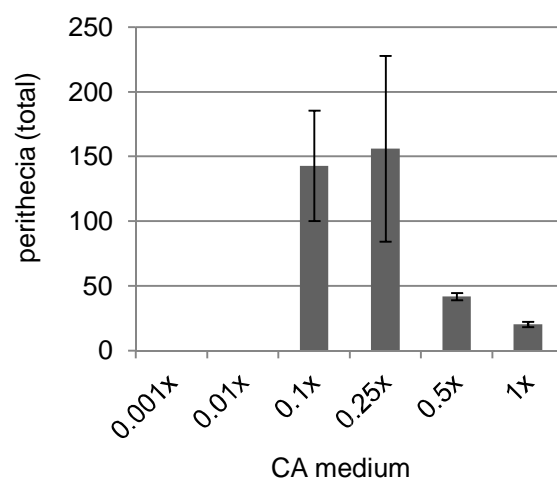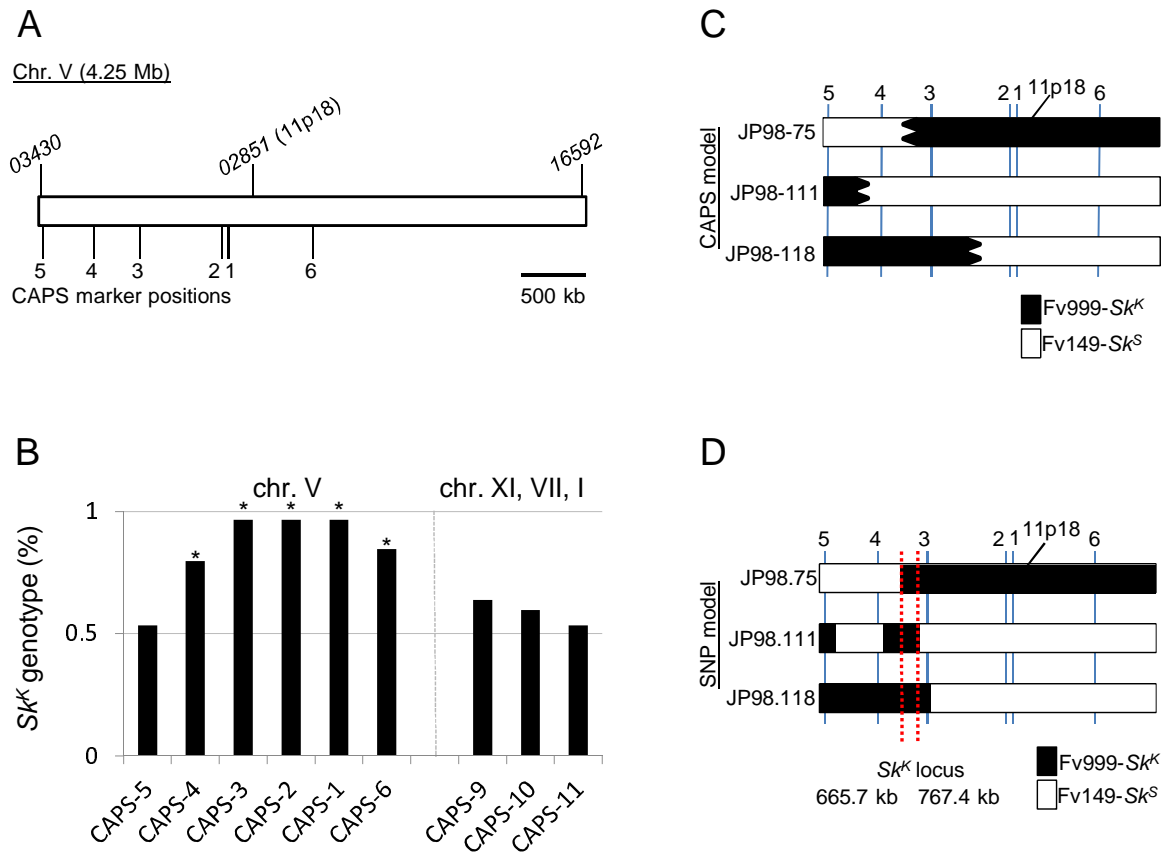
Figure 1

Figure 2

Figure 3
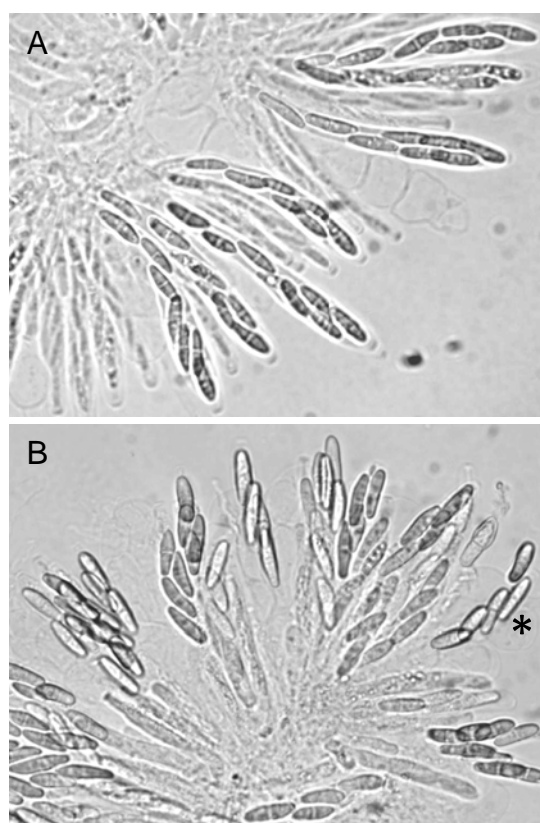
Figure 4
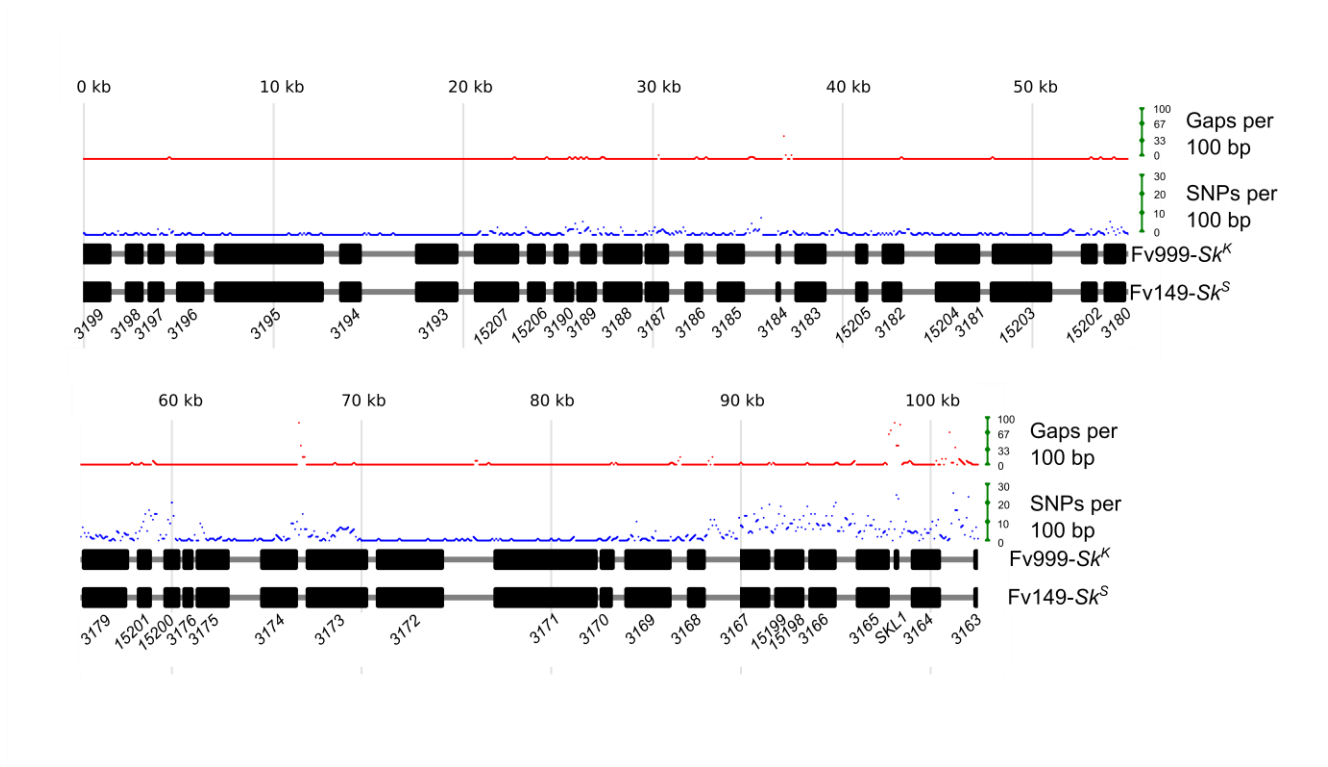
Figure 5
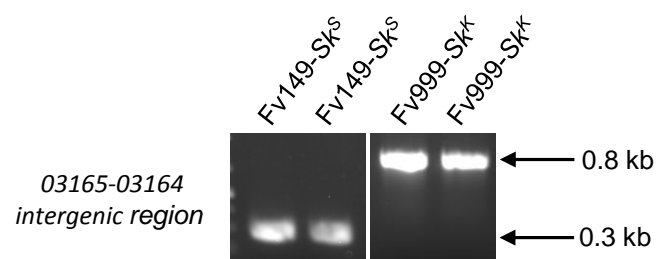
Table 1 Key strains used in this study

name[1]	genotype	alternate names
Fv149	Sk^S, *MAT-1*	FGSC 7600[2], M-3125[3], A00149[3]
Fv999	Sk^K, *MAT-2*	FGSC 7603[2], A00999[4]
RJP98.75	Sk^K, *MAT-2*	this study
RJP98.111	Sk^K, *MAT-2*	this study
RJP98.118	Sk^K, *MAT-2*	this study
RBM43.31	Sk^K, *MAT-1*	this study

Table 2 Draft genome assembly statistics

name	total[1]	contigs	avg. length[2]	# reads	N50	coverage[3]
Fv999-Sk^K	41,922,529	855	255	10,956,620	109,413	67
RPJ98.75-Sk^K	41,848,894	985	257	8,087,199	91,461	50
RPJ98.111-Sk^K	41,892,017	841	242	12,538,869	120,565	72
RPJ98.118-Sk^K	41,868,129	914	268	9,009,572	88,867	58

Table 3 Marker locations

marker	chromosome	position (Mb)
CAPS-1	V	1.47
CAPS-2	V	1.42
CAPS-3	V	0.78
CAPS-4	V	0.43
CAPS-5	V	0.02
CAPS-6	V	2.12
CAPS-9	XI	0.07
CAPS-10	VII	1.05
CAPS-11	I	0.73
RFLP-11p18	V	1.67

Table 4 Comparison of predicted protein-coding sequences within the *Sk* locus of Fv999-*Sk^k* and Fv149-*Sk^S*

name	Fv999-*Sk^K* length	Fv149-*Sk^S* length	alignment length	identity (%)	similarity (%)
3198	279	279	279	0.99	0.99
3197	224	224	224	0.99	0.99
3196	462	462	462	1.00	1.00
3195	1786	1786	1786	1.00	1.00
3194	359	359	359	1.00	1.00
3193	655	655	655	1.00	1.00
15207	634	666	692	0.93	0.94
15206	274	274	274	1.00	1.00
3190	146	242	242	0.99	1.00
3189	246	336	336	0.89	0.91
3188	599	599	599	0.99	1.00
3187	327	327	327	0.98	0.99
3186	234	234	234	1.00	1.00
3185	409	409	409	1.00	1.00
3184	65	46	65	0.96	0.98
3183	513	513	513	1.00	1.00
15205	174	174	174	0.99	1.00
3182	379	355	379	0.97	0.98
15204	88	88	88	1.00	1.00
3181	667	667	667	1.00	1.00
15203	1029	1085	1085	0.99	0.99
15202	194	194	194	1.00	1.00
3180	359	359	359	0.97	0.99
3179	784	736	784	0.97	0.97
15201	227	227	227	0.89	0.90
15200	288	288	288	0.93	0.98
3176	139	139	139	1.00	1.00
3175	496	496	496	0.99	1.00
3174	620	620	620	0.96	0.97
3173	964	964	964	0.97	0.98
3172	1018	1018	1018	1.00	1.00
3171	1724	1724	1724	1.00	1.00
3170	230	212	230	0.98	0.98
3169	716	716	716	0.99	0.99
3168	299	299	299	1.00	1.00
3167	460	460	460	0.97	0.98
15199	133	133	133	0.80	0.86
15198	323	319	323	0.93	0.95
3166	466	466	466	0.90	0.95
3165	532	531	532	0.98	0.99
SKL1	70	missing	na	na	na
3164	476	479	479	0.98	0.99

Table 5 Expression analysis of genes from the *Sk* locus during sexual development

ID	2 h	24 h	48 h	72 h	96 h	144 h	Min[1]	Max[2]	Fold change[3]
3198	39.17	150.92	38.40	24.98	28.10	20.10	20.10	150.92	7.51
3197	256.38	368.62	217.04	122.34	103.97	231.66	103.97	368.62	3.55
3196	0.83	0.13	0.87	0.56	0.83	0.87	0.13	0.87	6.59
3195	2.49	0.57	2.48	0.62	5.80	0.79	0.57	5.80	10.12
3194	0.25	0.12	0.30	14.02	124.53	1.20	0.12	124.53	1050.12
3193	138.42	94.82	71.69	43.35	80.19	75.41	43.35	138.42	3.19
15207	1.41	1.35	16.98	1.71	2.05	2.46	1.35	16.98	12.55
15206	0.78	1.40	5.23	1.29	0.76	1.08	0.76	5.23	6.86
3190	0.00	0.00	0.00	0.00	0.23	0.00	0.00	0.23	2.32
3189	0.00	0.00	0.00	0.05	0.50	0.00	0.00	0.50	4.95
3188	1.73	0.36	1.58	0.48	2.72	0.40	0.36	2.72	7.65
3187	1.90	0.97	1.34	31.36	42.16	0.71	0.71	42.16	59.47
3186	1.45	0.55	0.81	0.77	0.37	0.61	0.37	1.45	3.91
3185	5.41	3.74	6.17	2.61	1.72	1.51	1.51	6.17	4.09
3184	0.58	0.00	1.19	0.84	9.94	0.79	0.00	9.94	99.38
3183	59.62	22.63	32.99	13.12	29.15	21.10	13.12	59.62	4.54
15205	4.06	1.68	6.07	3.12	10.00	1.23	1.23	10.00	8.15
3182	0.30	0.00	1.19	0.00	0.29	0.00	0.00	1.19	11.93
15204	5.10	3.36	84.28	5.20	12.73	5.45	3.36	84.28	25.10
3181	2.16	0.50	5.24	0.50	1.93	0.66	0.50	5.24	10.57
15203	4.74	0.12	3.02	1.00	4.72	0.95	0.12	4.74	39.22
15202	1.05	0.44	8.61	7.61	9.45	0.74	0.44	9.45	21.57
3180	2.20	0.00	3.14	0.14	0.98	0.17	0.00	3.14	31.38
3179	1.28	0.06	1.14	0.10	2.70	0.09	0.06	2.70	47.85
15201	4.11	0.57	4.26	1.33	4.46	0.49	0.49	4.46	9.01
15200	1.02	0.55	0.32	0.36	0.29	0.24	0.24	1.02	4.16
3176	126.00	50.26	80.75	15.66	31.67	29.31	15.66	126.00	8.05
3175	48.87	12.93	38.03	9.13	19.60	13.41	9.13	48.87	5.35
3174	4.53	1.43	8.61	0.94	4.68	1.29	0.94	8.61	9.18
3173	1.04	0.17	2.86	0.42	1.90	0.42	0.17	2.86	17.29
3172	1.01	0.00	3.78	0.45	2.16	0.70	0.00	3.78	37.81
3171	2.95	37.34	38.55	117.07	44.37	94.58	2.95	117.07	39.66
3170	0.14	0.19	0.00	0.81	0.13	0.44	0.00	0.81	8.09
3169	5.48	0.61	5.38	3.02	7.40	2.61	0.61	7.40	12.05
3168	4.33	21.39	2.58	13.90	7.76	2.19	2.19	21.39	9.77
3167	0.17	0.71	0.13	0.21	0.12	0.04	0.04	0.71	19.47
15199	0.07	0.00	0.00	0.00	0.00	0.00	0.00	0.07	0.71
15198	1.34	0.12	0.56	0.21	0.31	0.19	0.12	1.34	11.68
3166	0.99	0.17	1.43	0.24	0.31	0.22	0.17	1.43	8.36
3165	20.77	11.51	13.49	9.68	8.41	4.09	4.09	20.77	5.07
SKL1	481.58	392.59	227.42	211.66	360.52	97.65	97.65	481.58	4.93
3164	16.11	30.78	16.09	6.78	16.48	15.70	6.78	30.78	4.54

Figure S1
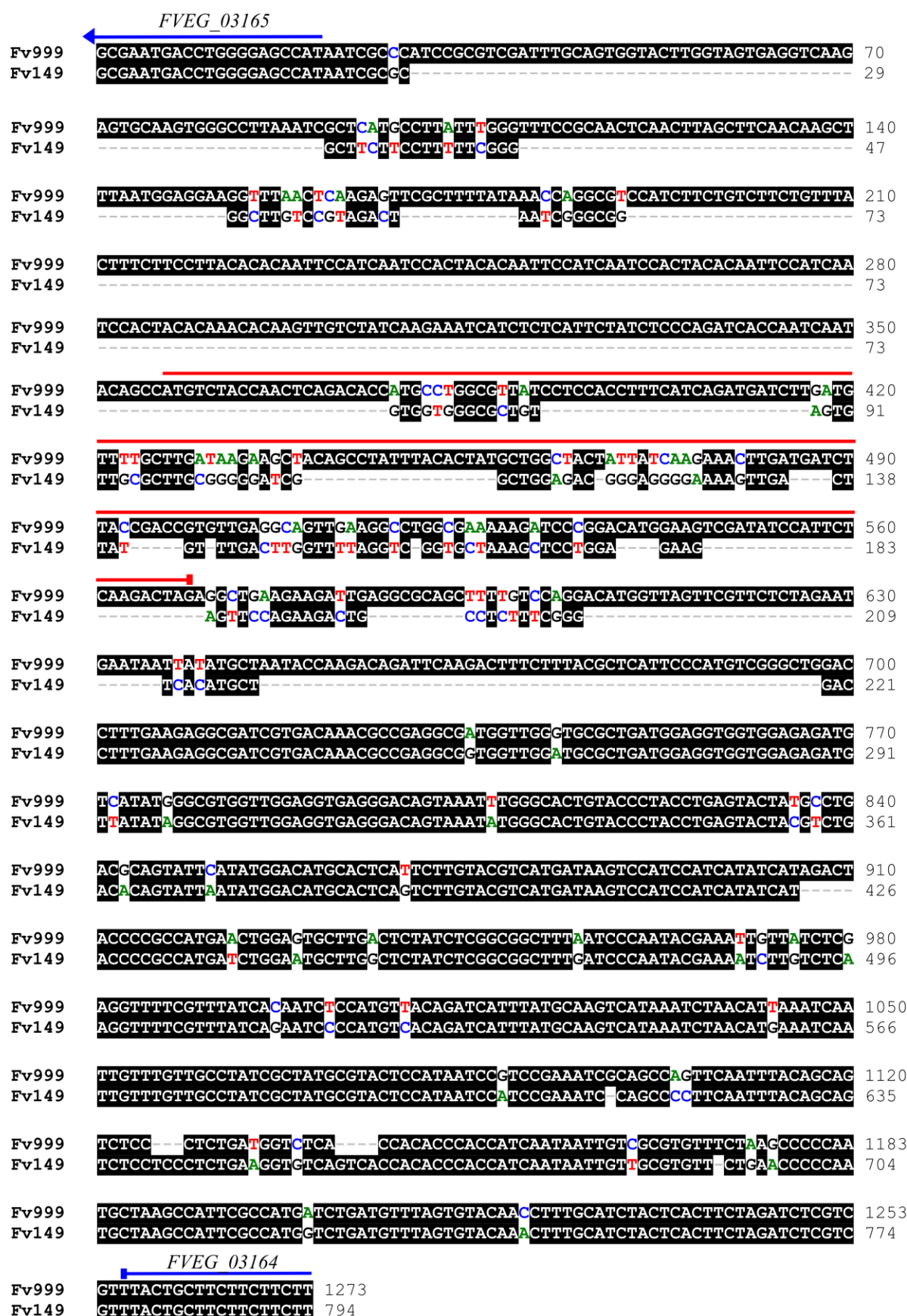
Table S1 Oligonucleotide primers for CAPS markers

Name	Sequence (5' to 3')
CAPS-1F	GCGATACAGAACCCCCATTCTCTT
CAPS-1R	GATCAGCCATCCTATCTCTCCCAGT
CAPS-2F	TTATCTGCACACCTGGAGGA
CAPS-2R	CGGCTTCACCTGAGACATTT
CAPS-3F	CCAGAATGGCTCTGACCTGGTGT
CAPS-3R	GCGCAGATCATGGAGAGGGTATG
CAPS-4F	ATGTGTGCAGCTCGTTTTTG
CAPS-4R	TCAACCCCGAGACTTTCATC
CAPS-5F	GACCAGACCCGAAACCAAT
CAPS-5R	CAGCCAAATCACGCTGTCT
CAPS-6F	GGTCGAGAACAAAGGGGTTC
CAPS-6R	CAAAGATGGGAGGAACATGG
CAPS-9F	CGCGGTTGACACGGCTCTC
CAPS-9R	GAAATGCGGCTCCAACTTCTCG
CAPS-10F	TGCTGCCTCGATTCCTTCTTCC
CAPS-10R	CGGAGTACCATTGTTCGGGTGA
CAPS-11F	TGCACAGAAGCGAGACAAACATCC
CAPS-11R	TCGAGCATGACCAAGGCAGAAC

Table S2 CAPS marker sizes

marker	PCR product length	Fv149 product lengths after *Hae*III digest	Fv999 product lengths after *Hae*III digest
CAPS-1	358	44, 86, 228,	151, 207
CAPS-2	307	132, 175	307
CAPS-3	311	311	105, 206
CAPS-4	288	110, 178	288
CAPS-5	265	119, 146	265
CAPS-6	325	34, 92, 199	34, 291
CAPS-9	291	128, 163	291
CAPS-10	404	404	68, 336
CAPS-11	333	333	108, 225

Table S3. Genotypes of the Fv999 (SK^K) × Fv149 (SK^S) mapping population at each CAPS location

Strain	CAPS-5	CAPS-4	CAPS-3	CAPS-2	CAPS-1	CAPS-6	CAPS-9	CAPS-10	CAPS-11
#60	S	K	K	K	K	K	K	K	K
#61	S	S	K	K	K	K	S	S	nd
#62	K	K	K	K	K	K	S	K	S
#63	K	K	K	K	K	K	K	K	S
#64	K	K	K	K	K	K	S	K	K
#65	K	K	K	K	K	K	S	K	S
#66	K	K	K	K	K	K	K	K	K
#67	S	K	K	K	K	K	S	S	S
#68	K	K	K	K	K	K	S	S	nd
#69	S	K	K	K	K	K	S	K	K
#70	S	K	K	K	K	K	nd	S	S
#71	S	S	K	K	K	K	nd	K	K
#72	K	K	K	K	K	K	K	S	S
#73	K	K	K	K	K	S	S	S	S
#74	K	K	K	K	K	K	K	K	K
#75	S	S	K	K	K	K	K	S	S
#76	S	K	K	K	K	K	K	S	S
#77	S	K	K	K	K	K	S	K	S
#78	K	K	K	K	K	K	S	K	K
#79	S	K	K	K	K	K	S	K	K
#80	S	S	K	K	K	K	S	K	K
#81	K	K	K	K	K	K	K	K	S
#82	S	K	K	K	K	K	K	K	K
#83	K	K	K	K	K	K	K	K	K
#84	S	K	K	K	K	K	K	K	S
#85	K	K	K	K	K	K	K	S	K
#86	K	K	K	K	K	K	K	K	K
#87	S	S	K	K	K	K	K	K	K
#88	S	nd	K	K	K	K	K	S	S
#89	S	K	K	K	K	K	K	S	K
#90	S	K	K	K	K	K	K	K	S

#91	K	K	K	K	K	K	K	K	K
#92	S	K	K	K	K	K	K	nd	K
#93	S	K	K	K	K	K	K	K	K
#94	S	K	K	K	K	S	K	K	S
#95	K	K	K	K	K	K	K	K	S
#96	K	K	K	K	K	K	S	K	S
#97	K	K	K	K	K	S	K	K	S
#98	K	K	K	nd	K	K	K	K	K
#99	K	K	K	K	K	K	K	S	S
#100	S	K	K	K	K	K	K	K	S
#101	S	S	K	K	K	K	K	S	K
#102	K	K	nd	K	K	K	S	K	K
#103	K	K	K	K	K	K	S	K	K
#104	S	K	K	K	K	S	S	S	S
#105	S	K	K	K	K	S	K	K	S
#106	S	S	K	K	K	S	S	S	S
#107	K	K	S	K	K	K	S	S	S
#108	K	S	K	K	K	K	K	nd	K
#109	K	K	K	K	K	K	K	K	S
#110	S	S	K	K	K	S	S	S	K
#111	K	S	S	S	S	S	K	S	K
#112	K	K	K	K	K	K	S	nd	K
#113	K	K	K	K	K	K	K	S	S
#114	K	K	K	K	K	K	K	S	S
#115	K	K	K	K	K	nd	S	S	K
#116	S	S	K	K	K	K	K	K	K
#117	K	K	K	K	K	K	K	S	K
#118	K	K	K	S	S	S	K	K	K
#119	S	S	K	K	K	K	K	S	K

The chromosome V CAPS markers (1 through 6) are arranged in the table according to their relative order on the chromosome. K = Fv999-Sk^K genotype; S = Fv149-Sk^S genotype; nd = not determined.